JOURNAL OF THERMOPHYSICS AND HEAT TRANSFER
Vol. 19, No. 4, October–December 2005

Recombination Coefficients and Spectral Emissivity of Silicon Carbide–Based Thermal Protection Materials

S. Pidan,* M. Auweter-Kurtz,† G. Herdrich,‡ and M. Fertig*
University of Stuttgart, 70550 Stuttgart, Germany

The method for determining the recombination coefficients for ceramic materials in air plasma and pure oxygen plasma is described. Additionally, a new method for the in situ determination of the spectral emissivity of high-temperature ceramic materials is presented. Values of the recombination coefficients for considered materials, resulting from the described methodology, are given at temperatures between 1483 and 1851 K and pressures between 356 and 950 Pa and compared with literature. Values of the spectral emissivities of the investigated materials are presented in a temperature range from about 1200 to 1820 K and compared with values obtained by other authors. Obtained results will be used for the development of catalytic sensors in the frame of the European reentry program EXPERT.

Nomenclature

A	=	area
a	=	transfer coefficient of pyrometer
b	=	linearity factor of pyrometer
c	=	specific heat
h	=	enthalpy
K	=	spectral emissivity correction factor
k	=	recombination rate, number of capacitor
L	=	spectral radiance
Le	=	Lewis number
M	=	molar mass
Ma	=	Mach number
$\dot{m}$	=	mass flow
n	=	coil windings
p	=	pressure
$\dot{q}$	=	heat flux
R	=	radius
$\Re$	=	universal gas constant
Sc	=	Schmidt number
s	=	thickness
T	=	temperature
U	=	inductively coil voltage
u	=	velocity
x	=	coordinate, axial distance
y	=	coordinate, radial distance
β	=	accommodation coefficient
γ	=	recombination coefficient
ε	=	emissivity
μ	=	dynamic viscosity
ξ	=	dissociation degree
ρ	=	density
σ	=	Stefan–Boltzmann constant
φ	=	quotient

Subscripts

amb	=	ambient pressure
c	=	cylinder
coil	=	inductively coil
D	=	dissociation
e	=	boundary layer edge
eff	=	effective
full_cat	=	fully catalytic
finite_cat	=	finite catalytic
O	=	atomic oxygen
p	=	at constant pressure
pl	=	plasma
s	=	stagnation
tot	=	total
w	=	wall, water
∞	=	freestream

Presented as Paper 2004-2274 at the AIAA 37th Thermophysics Conference, Portland, OR, 4–7 June 2004; received 14 September 2004; revision received 29 December 2004; accepted for publication 30 December 2004.

*Research Engineer, Department of Space Transportation Technology, Institut für Raumfahrtsysteme, Pfaffenwaldring 31.

†Professor, Department of Space Transportation Technology, Institut für Raumfahrtsysteme, Pfaffenwaldring 31.

‡Research Engineer, Department of Space Transportation Technology, Institut für Raumfahrtsysteme, Pfaffenwaldring 31. Member AIAA.

I. Introduction

THE catalytic efficiency of a thermal protection system (TPS) defines the finite catalytic reaction rates of gases in chemical nonequilibrium on the material's surface. During reentry of space vehicles into Earth's atmosphere, the airflow molecules (i.e., oxygen and nitrogen) passing through the bow shock become dissociated. The atoms can then recombine at different rates (depending on the catalytic efficiency of TPS materials) to molecules on the TPS surface or in the gas phase. Because of transfer of the recombination energy to the material surface, the heat flux on the reentry vehicle depends on catalytic efficiency of the TPS materials. Because the catalytic properties of these materials depend on temperature, the heat flux indirectly depends on the vehicle surface temperature and, consequently, on the thermal emissivity of the TPS materials. Therefore, for accurate prediction of thermal loads during reentry and for the lightweight design of the TPS, it is important to know both the catalytic efficiency and the emissivity of the material used.

Experimental investigations[1] show the temperature dependency of the oxygen and nitrogen recombination coefficients on investigated materials in the air plasmas, for example, on silicon carbide and silicon dioxide (quartz). Stewart[1] reported that silicon carbide (SiC) and borosilicate glass have maximum oxygen recombination coefficients. Both materials were investigated in a side-arm reactor and arcjet facilities. (SiC has a maximum at about 1330 K and glass at about 1600 K.) Moreover, the borosilicate glass also has a maximum nitrogen recombination coefficient value at about 1600 K.

The theoretical modeling done by Fertig et al.[2] predicts the peak values of recombination coefficients for SiC and quartz glass (SiO_2) for oxygen recombination. The peak values of $\gamma_{SiC(O)} = 0.2$–0.3 are typical for high-catalytic materials. In the low-temperature regions

(300–500 K) the values of $\gamma_{\mathrm{SiC}(O)}$ are about 10^{-3} (quite low), typical for medium catalytic materials.

This paper presents the investigation of five materials regarding their catalytic behavior in air plasma and pure oxygen plasma, namely sintered silicon carbide (SSiC), chemical-vapor-deposited silicon carbide (CVD-SiC) coating on the carbon/carbon silicon carbide (C/C-SiC) sample, yttrium silicate coating on the C/C-SiC sample, synthetically produced magnesium spinel, and oxidized aluminum. Additionally, investigations on SSiC, CVD-SiC coating, yttrium silicate coating, and spinel, referring to their spectral emissivity at 900 nm in air plasma, are described. The investigations of the C/C-SiC samples with CVD-SiC and yttrium silicate coatings were performed within the German space research program Ausgewählte Systeme und Technologien für zukünftige Raumtransportsystem-Anwendungen.

The catalytic experiments have been conducted with the magnetoplasmadynamic generator RD5[3,4] (qualitative comparison tests) in the plasma wind tunnel PWK2 and with the inductively heated plasma generator IPG3[3,4] (quantitative comparison tests) in the plasma wind tunnel PWK3 of the Institute of Space Systems (IRS) of the University of Stuttgart. The planned catalytic experiments with PWK3 in nitrogen and air plasmas will be conducted in the near future.

The emissivity investigations were conducted in the IRS PWK2 plasma wind tunnel, which is equipped with the RD5 magnetoplasmadynamic generator.

II. Determination of the Recombination Coefficients and Spectral Emissivity

This section describes the methods for determining the recombination coefficients in oxygen plasma flows and in situ determination of the spectral emissivities of the investigated materials.

A. Determination of Recombination Coefficients

The methodology used for determining the recombination coefficients of the investigated materials is similar to the methodology for determining the effective recombination coefficients in nitrogen and air plasmas used by Scott,[5] with the exception that the experiments at IRS for quantitative comparison of the catalytic behavior of the investigated materials have been conducted in pure oxygen plasma. The determination of the recombination coefficients has been carried out based on the Goulard's theory[6] and heat fluxes were measured for the investigated materials in the stagnation point in oxygen plasma flow. The recombination rate constant k_w (and the recombination coefficient γ_o) on the material surface can be determined from the ratio of the fully catalytic heat flux to the measured finite catalytic heat flux and under the assumption of complete accommodation of the released chemically energy (i.e., the energy accommodation coefficient, $\beta = 1$).

For the calculation of the fully catalytic heat flux, copper oxide (CuO) has been used as reference material, because other materials that could be highly catalytic and for which the literature data of the oxygen recombination coefficients can be found were not available for this work.

The fully catalytic heat flux $\dot{q}_{\mathrm{full\_cat}}$ was calculated with the heat flux $\dot{q}_{\mathrm{full\_cat}} = \dot{q}_{\mathrm{CuO}}$ measured on a cooled oxidized copper sample. With the known oxygen recombination coefficient of CuO, one can calculate the recombination rate constant $k_{w\mathrm{CuO}(O)}$ for the oxygen recombination on a CuO surface using

$$k_{w\mathrm{CuO}(O)} = \frac{2\gamma_{\mathrm{CuO}(O)}}{2-\gamma_{\mathrm{CuO}(O)}}\sqrt{\frac{\Re T_w}{2\pi M_O}} \tag{1}$$

$$\varphi = 1 \Bigg/ \left\{1 + \frac{0.665}{Sc^{\frac{2}{3}}\rho_w k_w}\left(\frac{u_\infty \mu_e \rho_e}{R_{\mathrm{eff}}}\right)^{0.5}\left[\frac{\rho_\infty}{\rho_e}\left(2-\frac{\rho_\infty}{\rho_e}\right)\right]^{0.25}\right\} \tag{2}$$

$$\dot{q}_{\mathrm{full\_cat}} = \dot{q}_{\mathrm{finite\_cat}}\left(1 - \frac{Le^{\frac{2}{3}}\xi_O\left(h_D^O/h_{\mathrm{se}}\right)}{1+(Le^{\frac{2}{3}}-1)\xi_O\left(h_D^O/h_{\mathrm{se}}\right)}\cdot[1-\varphi]\right)^{-1} \tag{3}$$

where the fully catalytic heat flux can be calculated. The dissociation degree ξ_O in the oxygen plasma flow at the measurement position has been determined to be very close to unity.[7]

In the next step, the heat flux measured on the investigated materials was used to calculate the recombination rate constant on the material surface from Eqs. (2) and (3) and eventually to calculate the recombination coefficient by using Eq. (1).

All plasma parameters (gas constant, density, etc.) at the boundary-layer edge and at the sample wall have been calculated under the assumption that the plasma at the boundary-layer edge and at the wall is in thermochemical equilibrium. Admittedly, this simplification results in erroneous values of some of the terms of Eqs. (2) and (3), which lead to discrepancies in values of recombination coefficients. However, the assessment of the influence of the equilibrium assumption for calculation of plasma parameters leads to values of recombination coefficients of the same order of magnitude. Schmidt and Lewis numbers and viscosity values have been calculated according to Ref. 8.

For the calculation of the local stagnation enthalpy at boundary-layer edge h_{se}, the following equation was used[7]:

$$\frac{h_{\mathrm{se}}(x,0)}{h_{\mathrm{tot}}} \approx \frac{R_{\mathrm{pl}}^2}{2}\left[\frac{\dot{q}(x,0)}{\sqrt{p_{\mathrm{pitot}}(x,0)}} \Bigg/ \int_0^{R_{\mathrm{pl}}} \frac{\dot{q}(x,y)}{\sqrt{p_{\mathrm{pitot}}(x,y)}}\, y\, \mathrm{d}y\right] \tag{4}$$

where $R_{\mathrm{pl}} = 100$ mm.

The total flow enthalpies h_{tot} were measured with a cavity calorimeter[7] and the radial profiles of the heat flux and pitot pressure were measured with the double probe for the heat flux and pitot pressure measurements (Fig. 1).[7]

To calculate plasma speed u_∞, Mach number Ma_∞ and the effective isentropic exponent κ_∞ are needed. Their values were obtained from the pitot and ambient pressure measurements and from the measurements with the wedge probe[7] (Fig. 2). The measurements

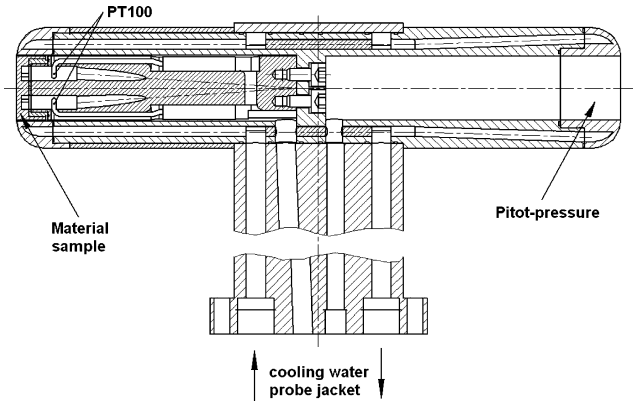

Fig. 1 Double probe for the heat flux (calorimetric) and pitot-pressure measurements.

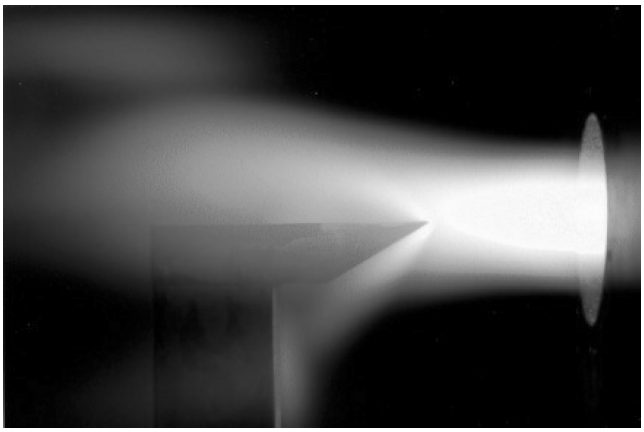

Fig. 2 Wedge probe in operation (PWK3, IPG3): condition 1, distance from IPG3 is 210 mm.

Table 1 Test conditions with RD5/PWK2

Condition	Gas mass flow	p_∞, Pa	p_{pitot}, Pa	RD5 current, A	Distance from RD5, mm
1	2 g/s air (0.47 g/s O_2; 1.53 g/s N_2) + 0.3 g/s argon	20	60	1258	450
2	8 g/s air (1.86 g/s O_2; 6.14 g/s N_2) + 0.3 g/s argon	490	660	1071	730

Table 2 Test conditions with IPG3/PWK3

Condition	Gas mass flow, g/s O_2	k	n	p_∞, Pa	p_{pitot}, Pa	U_{coil}, V	Distance from IPG3, mm
1	3	4	5.5	40	Variable	6300	90, 120, 150, 180
2	3	4	5.5	500	950	6300	393

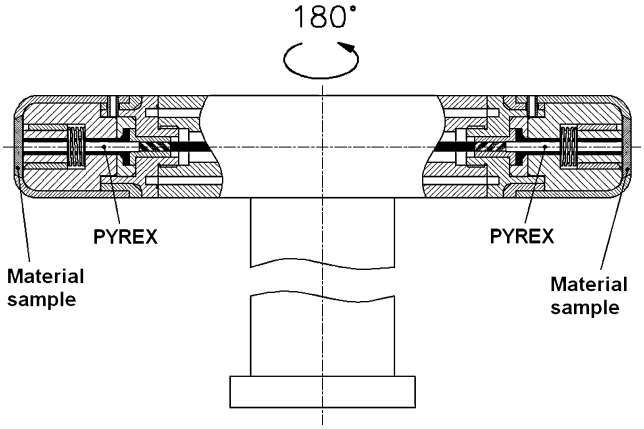

Fig. 3 Material double probe with Pyrex minipyrometers.

with the wedge probe allow the Mach number to be defined from the oblique shock relation for the deflection and shock angles.

The effective radius of the probe has been estimated using two calculations performed with the URANUS code[9] under the same freestream condition for the standard IRS sample holder (cylinder diameter = 50 mm) and for a hemispherical blunt body (hemispherical radius = 25 mm). The freestream conditions are $Ma_\infty = 4$, $p_\infty = 40$ Pa, and $h_\infty = 34$ MJ/kg. The value of the effective radius has been estimated as $R_{\text{eff}} = 2.42R_c$, where R_c is the cylinder radius of the sample holder. This is not in agreement with the data from Mizuno et al.,[10] who used the relation obtained by Boison and Curtiss.[11] The data used by Mizuno have following relations: at $Ma_\infty = 2.01$, $R_{\text{eff}} = 2.9R_c$; at $Ma_\infty = 4.76$, $R_{\text{eff}} = 3.7R_c$. The possible reason for this difference can be other pressure levels and, consequently, other flow Knudsen numbers.

B. Heat Flux Measurements

Heat flux measurements have been conducted with two probes developed at IRS: a calorimetric heat flux–pitot-pressure double probe (Fig. 1) and the material double probe[12] (Figs. 3 and 4).

Because water is a good heat capacitor, it has been used for calorimetric heat flux measurements on the cooled samples. With the measured temperature difference in the inlet and outlet of cooling water flows, one can calculate the heat flux on the sample:

$$\dot{q}_{\text{sample calor.}} = c_{\text{pw}}\dot{m}(T_{\text{outlet}} - T_{\text{inlet}})/A_{\text{sample}} \tag{5}$$

The temperature measurements of the cooling water flows are performed with two resistance thermometers of type PT100. The resistance thermometers are placed as close as possible to the water-cooled surface.

Heat flux measurements on a copper sample oxidized under a temperature of about 450°C and on an aluminum sample oxidized in the oxygen plasma flow have been taken by using the calorimetric heat flux and pitot-pressure double probe. The temperature of these samples was about 300 K during the tests.

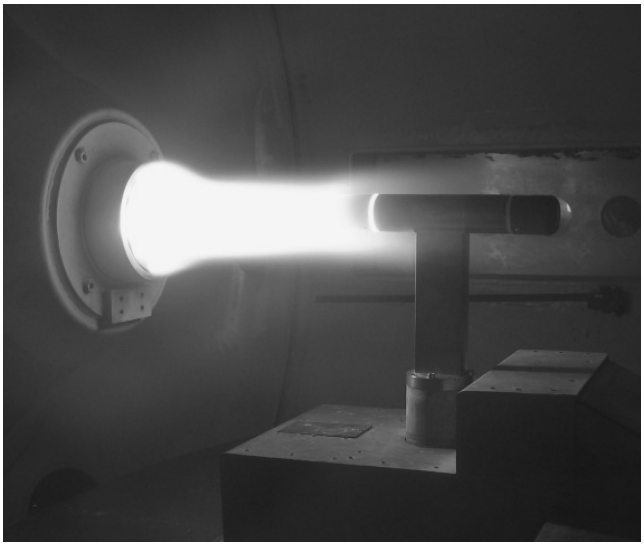

Fig. 4 Material double probe in operation (PWK2, RD5).

Heat flux measurements on SSiC, CVD-SiC, yttrium silicate coating, and synthetically produced magnesium spinel have been performed with the material double probe. This probe is equipped with two Pyrex[13] minipyrometers for the temperature measurement of the rear side of the sample. During the experiments the material double probe is brought into the plasma flow and stays there until the sample temperature has reached a constant value. Due to high-temperature thermal insulation between sample and probe, the rear side of the sample can be assumed to be adiabatic. Neglecting ambient temperature, the heat flux on the sample with a temperature of $T_w(t)$ can be estimated, employing the thin-wall method:

$$\dot{q}_{\text{sample}} \approx \varepsilon\sigma T_w^4(t) + c_p\rho s\frac{\mathrm{d}T_w(t)}{\mathrm{d}t} \tag{6}$$

where ε is the total emissivity of the material sample. The advantage of the material double probe is that two samples of different materials can be tested in one experiment and under the same test conditions by turning the probe 180 deg in the plasma wind tunnel. The design of the material double probe allows transient heat flux measurements.

C. In Situ Measurements of Spectral Emissivity

The in situ measurements of the spectral emissivity have been performed in the PWK2 plasma wind tunnel with the RD5 magnetoplasmadynamic generator. Material samples have been placed in the material double probe and the temperature T_1 of the rear side of the samples has been measured by Pyrex sensors during experiments. Because of the geometric shape and the placement of the ceramic tube behind the material sample (cavity is formed), the measured temperature of the sample's rear side does not depend on its emissivity. In this case the effective emissivity is almost equal to unity. The measurement with an external linear pyrometer and spectral

emissivity value equal to ε_2 would deliver an incorrect value of T_2. By adjusting the emissivity value on the external pyrometrical device until the temperature measured by the external pyrometer and the Pyrex measured temperature are the same (as soon as the sample temperature has reached a constant value), it is possible to correct the emissivity value. By using the external pyrometer with a defined measuring wavelength (e.g., to avoid the radiation bands of plasma), the spectral emissivity of the investigated materials can be defined in this way (also depending on the surface temperature). It should be noted that for correctly determining the spectral emissivity value the transfer function of the external pyrometer is required, because only the linearity of the spectral radiance L and pyrometer output voltage U is given. With the known transfer function of the pyrometer, $U = f(T)$, given by the manufacturer of the pyrometrical device, one can calculate the corrected emissivity values of the investigated material sample with following relation:

$$K = \frac{U_{\text{corr}}(T_1)}{U_2(T_2)} = \frac{L(T_1)\cdot b_{\text{corr}}}{L(T_1)\cdot b_2} = \frac{L(T_1)\cdot a/\varepsilon_{\text{corr}}}{L(T_1)\cdot a/\varepsilon_2}$$

$$= \frac{\varepsilon_2}{\varepsilon_{\text{corr}}} \Rightarrow \varepsilon_{\text{corr}} = \frac{\varepsilon_2}{K} \tag{7}$$

The transfer function of the pyrometrical device has been approximated with a fifth-degree polynomial function. With the temperature measurement uncertainty of $\pm 1.5\%$ (given by the manufacturer[14]), the error of the spectral emissivity determination is estimated as $\pm 11.3\%$.

Because the pyrometer has only one measuring wavelength equal to 900 nm, the spectral emissivity is investigated only at this wavelength.

III. Test Conditions

The experiments in the PWK3 plasma wind tunnel have been conducted in pure oxygen plasma under the following conditions.

Figure 5 shows the stagnation enthalpy profiles calculated with Eq. (4) for PWK3 test condition 1 (y is the radial distance from flow symmetry axis). Stagnation enthalpy for PWK3 test condition 2 was calculated as 10 MJ/kg, and the Mach number as 1.05. The Mach number and the pitot pressure for both test conditions in PWK3 are given in Fig. 6. One can see from Fig. 6 that both PWK3 test conditions are supersonic.

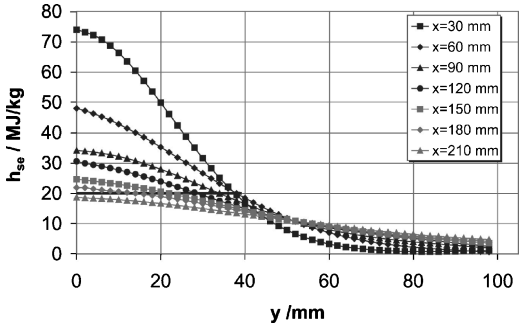

Fig. 5 Stagnation enthalpy profiles in PWK3 at condition 1.[7]

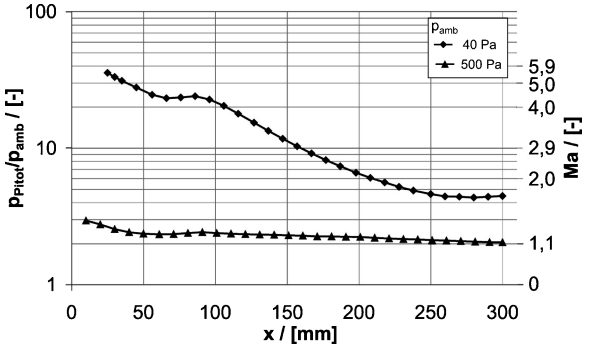

Fig. 6 Pressure and Mach number values for PWK3 tests.[7]

During each test the probes were driven into the middle of the plasma flow along the flow symmetry axis to change the distance to the plasma generator and to obtain the axial profiles of the temperatures or stagnation pressures.

IV. Test Results

A. Catalytic Properties

Catalytic properties of the materials used have been compared qualitatively with results from the experiments conducted in the PWK2 plasma wind tunnel at conditions shown in Table 1. The quantitative comparison of the catalytic activities of the investigated materials was done with the heat flux and plasma characteristic value measurements performed in the PWK3 plasma wind tunnel at conditions presented in Table 2. The methodology described in Sec. II was applied to calculate the recombination coefficients for oxygen.

1. Qualitative Comparison

The measured values of the heat fluxes on the different materials obtained in the PWK2 plasma wind tunnel allow the qualitative comparison of the catalytic behavior of the investigated materials. Figure 7 shows the heat flux histories of four materials, namely SSiC, spinel, C/C-SiC with CVD-SiC coating, and C/C-SiC with yttrium silicate coating. These measurements have been performed under condition 1 in PWK2 with RD5. In Fig. 8, the heat fluxes vs time on the same materials under condition 2 are given.

As expected, the results demonstrate approximately identical heat fluxes on the SSiC and C/C-SiC with CVD-SiC coating. The heat flux on the spinel is clearly lower than that on the SSiC, whereas the heat flux on the C/C-SiC with yttrium silicate coating is higher than that on the silicon carbide. These facts indicate that spinel should be less catalytic in air than silicon carbide; the yttrium silicate should be more catalytic vs air than SSC.

However, during the tests the steady-state temperature of the spinel sample was higher than the steady-state temperature of the SSiC sample, whereas the heat flux on spinel was much lower than that on SSiC. This difference in temperature is caused by the difference in total emissivity of both materials. In this temperature range

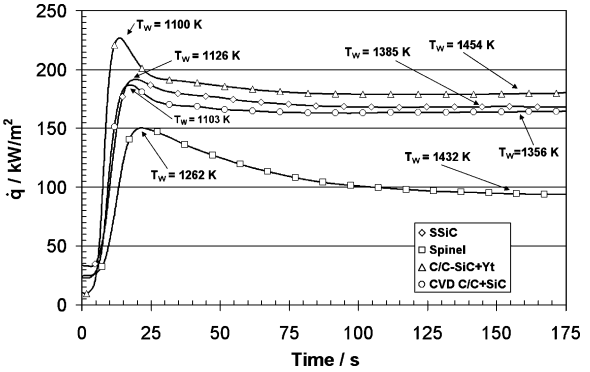

Fig. 7 Heat flux history of the investigated materials under condition 1 (PWK2, RD5).

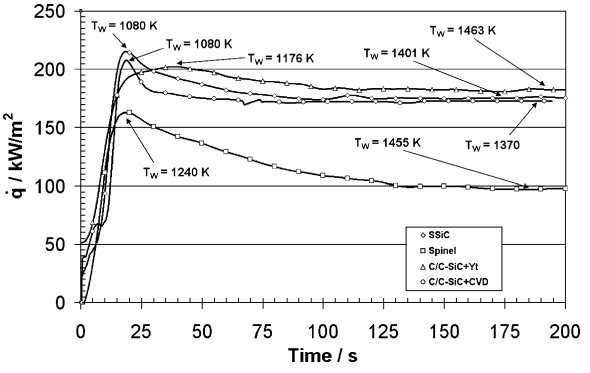

Fig. 8 Heat flux history of the investigated materials under condition 2 (PWK2, RD5).

spinel has a total emissivity value of about 0.4,[15] whereas the SSiC's value is about 0.8.[16] This shows the important role of the total surface emissivity. In spite of the low heat fluxes, caused, for example, by low catalytic activities of the material, the surface temperature can be quite high because of the low emissivity value.

In Figs. 7 and 8 the values of the heat fluxes are calculated using Eq. (6). Here the peak values are considered as total heat flux values for the investigated materials. These values attenuate with time because the heat flow in the probe's structure becomes noticeable. The difference between the heat flux peaks on spinel and SSiC at condition 1 is greater than this at condition 2, although the sample's surface temperatures at both conditions are approximately equal. A possible reason for this might be the lower dissociation degree of the plasma flow at condition 2 because of the greater distance from the plasma source.

2. *Quantitative Comparison*

The quantitative comparison of oxygen recombination coefficients has been done for three materials, namely SSiC, spinel, and oxidized aluminum. For the calculations of the oxygen recombination coefficients of the investigated materials, the oxygen recombination coefficient of the reference material (i.e., oxidized copper assumed as CuO) has to be known. The literature values for the copper oxide recombination coefficient have been found at room temperature as two values: 0.15 (Ref. 17) and 0.045 (Ref. 18). Because these values differ by about a factor of 3, which might lead to miscalculations, the recombination coefficient calculations for the investigated materials have been performed with both values.

In Fig. 9 the calculated values of the oxygen recombination coefficients of SSiC (labeled as SiC), together with values from other sources,[1,19] are shown. These values have been calculated using the heat flux measurements in pure oxygen plasma in PWK3. The error bars mark the deviations of about 60% of the calculated values of the recombination coefficients. This follows from Eqs. (2) and (3) together with the errors of the heat flux measurements. These errors lie at approximately 12% of the measured heat flux values.

The calculated values of the oxygen recombination coefficients for SSiC at 1650 K are about two to three times greater than values obtained at approximately the same temperature by Stewart in the arcjet facility.[1] The temperature dependence of the oxygen recombination coefficients of the SSiC is evident from Fig. 9.

The oxygen recombination coefficients of spinel have been calculated in the same way as those for SSiC. Figure 8 shows the values of γ_O for these materials (in Fig. 10 SSiC is labeled as SiC). Unfortunately, measurement at only one position in PWK3 in pure oxygen plasma with spinel is available at the present. In spite of this, and even with some different temperature values of the samples during the tests at the measured positions, one can see from the measurements with air in PWK2 (see Figs. 7 and 8) and from the oxygen recombination coefficient value obtained from PWK3 that the synthetically produced magnesium spinel used in this experiment should have lower catalytic activity for oxygen atoms than SSiC.

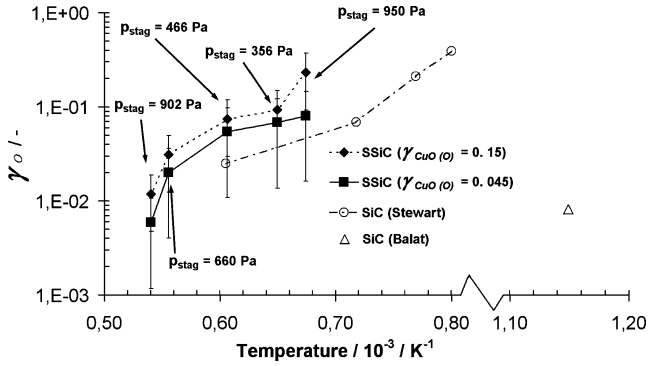

Fig. 9 Oxygen recombination coefficients of SSiC with stagnation pressure values: conditions 1 and 2 (PWK3, IPG3).

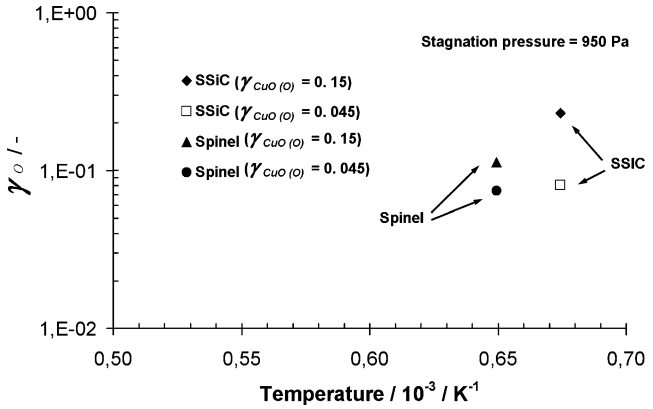

Fig. 10 Oxygen recombination coefficients of SSiC and spinel: condition 2 (PWK3, IPG3).

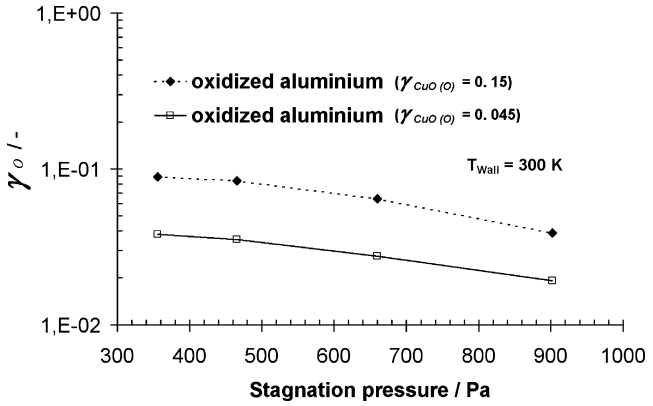

Fig. 11 Oxygen recombination coefficients of oxidized aluminum: condition 1 (PWK3, IPG3).

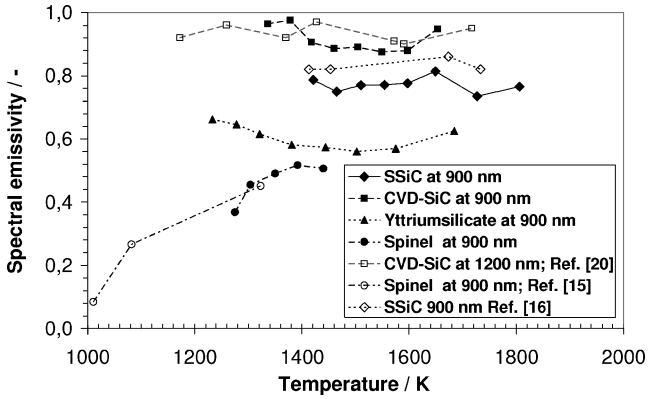

Fig. 12 Spectral emissivity values of the tested materials (PWK2, RD5).

During the experiments with the oxidized aliminum sample in pure oxygen plasma in PWK3, the sample's temperature was almost constant and had a value of about 300 K. The heat fluxes measured on the oxidized aluminum sample lie between the values of the heat fluxes on copper oxide and SSiC. Figure 11 gives the oxygen recombination coefficients of oxidized aluminum over the stagnation pressure. A pressure dependency of the oxygen recombination coefficients of the oxidized aluminum can be seen, whereas the pressure dependency becomes weak toward the low pressures.

B. Spectral Emissivity

The measurements of the spectral emissivity of the investigated materials were performed in the PWK2 facility equipped with the RD5 magnetoplasmadynamic generator. The methodology

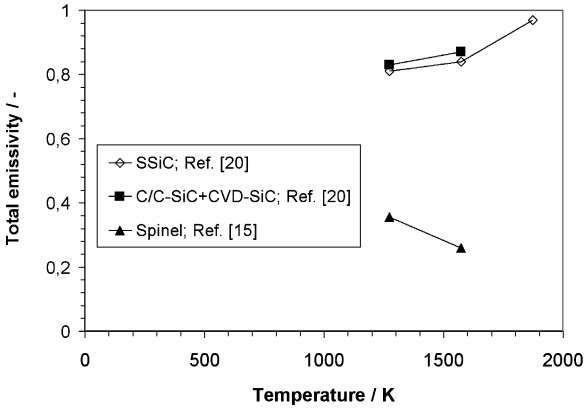

Fig. 13 Total emissivity values of the tested materials.

for determining the spectral emissivity values is described in Sec. II.

Figure 12 shows the measured values of the spectral emissivity values of the SSiC, CVD-SiC, spinel, and CVD yttrium silicate in comparison to values form other sources. The method used can be considered to give good agreement with the methods employed by other authors.[15,16,20]

The total emissivities of the investigated materials are shown in Fig. 13. The total emissivity of yttrium silicate layer was estimated independent from temperature as 0.7.

V. Conclusions

Within the frame of this work, a methodology for determining the recombination coefficients of ceramic materials such as SSiC, synthetically produced magnesium spinel, yttrium silicate, and CVD SiC, in a wide range of temperatures and metallic materials (oxidized aluminum) at a constant temperature of 300 K has been adapted. The tests conducted in air plasma under two conditions obtained with the RD5 magnetoplasmadynamic generator show that qualitative comparison between the catalytic activities of the investigated materials is possible. In addition, the experiments performed under two conditions with help of the inductively heated plasma source, IPG3, in pure oxygen plasma confirm the tests with air plasma in regard to the catalytic activities of the tested materials.

By using the employed methodology, the values of oxygen recombination coefficients of the investigated materials have been calculated. The calculated values of oxygen recombination coefficient for the SSiC at temperatures between 1483 and 1851 K lie in the range from 0.012 to 0.23. These values are in reasonable agreement with Stewart's data.[1] Further improvement is necessary for determination of boundary-layer and sample wall ambient conditions.

The methodology for the in situ determination of the spectral emissivities of ceramic materials has been proposed. The following ceramic materials have been investigated: SSiC, CVD-SiC, spinel, and yttrium silicate. The obtained values of the spectral emissivities at 900 nm for SSiC lie at about 0.8, for CVD-SiC at about 0.9, for yttrium silicate at about 0.6, and for spinel at about 0.5.

Further investigations concerning the determination of recombination coefficients are planned. The results of these investigations will be used for experiments in the framework of the European reentry program EXPERT.

Acknowledgments

The authors thank the DLR for support within the German space research program ASTRA. Special thanks go to Juergen Haeberle for excellent cooperation during the catalytic and emissivity measurement programs.

References

[1]Stewart, D. A., "Determination of Surface Catalytic Efficiency for Thermal Protection Materials—Room Temperature to Their Upper Use Limit," AIAA Paper 96-1863, June 1996.

[2]Fertig, M., Frühauf, H.-H., and Auweter-Kurtz, M., "Modelling of Reactive Processes at SiC Surfaces in Rarified Nonequilibrium Airflows," AIAA Paper 2002-3102, June 2002.

[3]Herdrich, G., Auweter-Kurtz, M., Endlich, P., Kurtz, H., Laux, T., Löhle, S., Nazina, N., Pidan, S., Schreiber, E., Wegmann, T., and Winter, M., "Atmospheric Entry Simulation Capabilities at IRS," *Proceedings of the 3th International Symposium Atmospheric Reentry Vehicles and Systems*, Association Aeronautique et Astronautique de France, March 2003.

[4]Herdrich, G., Löhle, S., Auweter-Kurtz, M., Endlich, P., Fertig, M., Pidan, S., and Schreiber, E., "IRS Ground Testing Facilities: Thermal Protection System Development, Code Validation and Flight Experiment Development," AIAA Paper 2004-2596, June–July 2004.

[5]Scott, C. D., "Catalytic Recombination of Nitrogen and Oxygen on High-Temperature Reusable Surface Insulation," AIAA Paper 80-1477, July 1980.

[6]Goulard, R., "On Catalytic Recombination Rates in Hypersonic Stagnation Heat Transfer," *Jet Propulsion,* Vol. 28, Nov. 1958, pp. 735–745.

[7]Herdrich, G., "Aufbau, Qualifikation und Charakterisierung einer induktiv beheizten Plasmawindkanalanlage zur Simulation atmosphärischer Eintrittsmanöver," Ph.D. Dissertation, Inst. of Space Systems, Univ. of Stuttgart, Stuttgart, Germany, 2004.

[8]Fertig, M., Dohr, A., and Fruehauf, H.-H., "Transport Coefficients for High-Temperature Nonequilibrium Air Flows," *Journal of Thermophysics and Heat Transfer*, Vol. 15, No. 2, 2001, pp. 148–156.

[9]Frühauf, H.-H., Fertig, M., Olawsky, F., Infed, F., and Bönisch, T., "Upwind Relaxation Algorithm for Reentry Nonequilibrium Flows," *High Performance Computing in Science and Engineering 2000*, Springer, Berlin, 2001, pp. 440–445.

[10]Muzino, M., Morino, Y., and Yoshinaka, T., "Evaluation of Reaction Rate Constants for Thermal Protection Materials in Dissociated Air Flow," AIAA Paper 99-3630, June–July 1999.

[11]Boison, J. C., and Curtiss, H. A., "An Experimental Investigation of Blunt Body Stagnation Point Velocity Gradient," *American Rocket Society (ARS) Journal*, Vol. 6, Feb. 1952, pp. 130–135.

[12]Pidan, S., Auweter-Kurtz, M., Herdrich, G., and Laux, T., "Experimentelle Erprobung eines Katalyzitätsbasierten Sensorsystems für die Wärmestromdichtemessungen im Plasmawindkanal SCIROCCO," *DGLR Jarestagung*, Bonn, Nov. 2003.

[13]Auweter-Kurtz, M., Fertig, M., Herdrich, G., Laux, T., Schöttle, U., Wegmann, Th., and Winter, M., "Entry Experiments at IRS—In-Flight Measurement During Atmospheric Entries," *Space Technology Journal*, Vol. 23, No. 4, 2003, pp. 217–234.

[14]Maurer, "Non-contact Temperature Measurement," Technical Brochure, GmbH, Kohlberg, Germany.

[15]Neuer, G., "Messung des Gesamtemissionsgrads und des spektralen Emissionsgrads an Spinell," IKE, IKE 5TB 207 GN-0212, Institut für Kernenergetik und Energiesysteme, Univ. of Stuttgart, Stuttgart, Germany, Dec. 2002.

[16]Lippmann, W., Nöring, R., and Umbreit, M., "Hochtemperaturverhalten SSiC-gekapselter UO_2-Pellets und Absorberelemente," Abschlussbericht, Technical Univ. of Dresden, Dresden, Germany, Feb. 2001.

[17]Hartunian, R. A., Thompson, W. P., and Safron, S., "Measurements of Catalytic Efficiency of Silver for Oxygen Atoms and the O-O_2 Diffusion Coefficient," *Journal of Chemical Physics,* Vol. 43, No. 11, 1965, pp. 4003–4006.

[18]Dickens, P. G., and Sutcliffe, M. B., "Recombination of Oxygen Atoms on Oxide Surfaces," *Transactions of the Faraday Society*, Vol. 60, Feb. 1964, p. 1272.

[19]Balat, M., Czerniak, M., and Badie, J. M., "Thermal and Chemical Approaches for Oxygen Catalytic Recombination Evaluation on Ceramic Materials at High Temperature," *Applied Surface Science*, Vol. 120, 1997, pp. 225–238.

[20]Brandt, R., Weiland, G. J., and Neuer, G., "Thermisches Verhalten von C/C-SiC" Interner Bericht, SFB 259, Teilprojekt B3, Institut für Thermodynamik der Luft- und Raumfahrt, Univ. of Stuttgart, Stuttgart, Germany.